doi.org/10.36721/PJPS.2026.39.7.198.1

Identification of putative inhibitors of human pancreatic α-amylase from phytochemicals using molecular docking and computational analysis

Mujahid Jalal[1], Muhammad Hasnat[1], Ayisha Khalid[2], Talha Ali Chohan[3]*, Ashfaq Ahmad[4], Ayesha Riaz[3], Sobia Alyas[3], Muhammad Shoaib Ali Gill[1], Umair Khurshid[5], Anjum Khursheed[6], Tahir Ali Chohan[1], Sirajudheen Anwar[7,8]* and Hammad Saleem[1]*

[1]Institute of Pharmaceutical Sciences (IPS), University of Veterinary and Animal Sciences (UVAS), Lahore, Pakistan
[2]Faculty of Pharmacy and Health Sciences, University of Balochistan, Quetta, Pakistan
[3]Institute of Molecular Biology and Biotechnology, The University of Lahore, Pakistan
[4]Department of Pharmacy Practice, College of Pharmacy, University of Hafr Al Batin, Saudi Arabia
[5]Department of Pharmaceutical Chemistry, Faculty of Pharmacy, The Islamia University of Bahawalpur, Pakistan.
[6]Faculty of Pharmacy, Grand Asian University, Sialkot, Pakistan
[7]Department of Pharmacology and Toxicology, College of Pharmacy, University of Hail, Hail, Saudi Arabia
[8]Saveetha Dental College and Hospitals, Saveetha Institute of Medical and Technical Sciences (SIMATS), Saveetha University, Chennai, Tamil Nadu, India.

Abstract: **Background**: Diabetes mellitus is a global chronic metabolic disorder characterized by elevated blood glucose levels, primarily due to impaired insulin activity or secretion. α-amylase, a key enzyme in carbohydrate digestion, is a validated molecular target for controlling postprandial hyperglycemia in type 2 diabetes. **Objectives**: This study aimed to identify potential α-amylase inhibitors from phytochemicals derived from *Bauhinia forficata*, Citrus spp. and *Echinops ritro* using an *in-silico* approach. **Methods**: A total of 55 phytochemicals were virtually screened against human pancreatic α-amylase (PDB ID: 3BAJ) using molecular docking via Schrödinger Maestro (version 12.5). The top-ranked ligands were further assessed for pharmacokinetic and toxicity profiles using SwissADME, ProTox-II and StopTox platforms. Electronic reactivity was evaluated using Density Functional Theory (DFT) with Gaussian 09. **Results**: Among the screened compounds, kaempferitrin (-10.3 kcal/mol), Rutin (-10.1 kcal/mol), Naringin (-9.7 kcal/mol) and Hyperoside (-9.6 kcal/mol) demonstrated strong binding affinities, favorable pharmacokinetic properties and compliance with drug-likeness criteria. DFT analysis supported their chemical reactivity and stability, indicating potential for biological activity. **Conclusion**: The results suggest that these phytochemicals could serve as promising lead molecules for the development of plant-based antidiabetic drugs targeting α-amylase. However, further experimental validation and mechanistic studies are recommended to confirm these findings.

Keywords: ADMET; Antidiabetic; α-amylase inhibition; DFT; Molecular docking; Phytochemicals

Submitted on 21-01-2025 – Revised on 17-07-2025 – Accepted on 02-09-2025

INTRODUCTION

The most prevalent hormonal disease is diabetes mellitus (DM). It is characterized by inadequate or insufficient insulin production by the pancreas, resulting in fluctuations in blood glucose levels. Diabetes mellitus is classified into two categories: Type II non-insulin-dependent diabetes mellitus (NIDDM) and Type I insulin-dependent diabetes mellitus (IDDM) (Kumar *et al*., 2020). Type I diabetes is an autoimmune disease characterized by an inflammatory response centered in and around the islets of Langerhans. The characteristics of type II diabetes include diminished insulin production and peripheral insulin resistance (Tomic *et al*., 2022). International Diabetes Federation (IDF) Atlas 10th Survey states that each year, 4 million individuals die from diabetes. 537 million people, or one in ten, are affected by diabetes (20-79 years old). This number is projected to rise to 643 million by 2030 and 783 million by 2045. One death every five seconds, or 6.7 million deaths, will be attributable to diabetes in 2021. Diabetes has caused health costs to increase by at least USD 966 billion, or 316%, during the preceding 15 years (Wang *et al*., 2022). The primary objectives of diabetes medications are life preservation and symptom relief; secondary objectives include averting long-term consequences and extending life expectancy by reducing risk factors (Classification and Diabetes, 2020). Insulin replacement treatment is critical for IDDM and dietary and lifestyle modifications are critical for NIDDM management. Biguanides (e.g., metformin) and sulfonylureas (e.g., glibenclamide) are among the most commonly used hypoglycemic agents in NIDDM treatment. However, these medications are associated with several adverse effects. For instance, metformin can cause gastrointestinal discomfort, lactic acidosis (in rare cases) and vitamin B12 deficiency with prolonged use (Mehrpour *et al*., 2022).

Historically, plant-based medications have been a consistent source. Well-studied examples include *Gymnema sylvestre*, known for regenerating pancreatic

**Corresponding author:* e-mail: hammad.saleem@uvas.edu.pk; si.anwar@uoh.edu.sa; talha.ali@imbb.uol.edu.pk

beta cells; *Momordica charantia* (bitter melon), which exhibits insulin-like activity; *Trigonella foenum-graecum* (fenugreek), which enhances glucose tolerance; and Ficus bengalensis, reported to have significant hypoglycemic effects. There is a wealth of evidence supporting the therapeutic use of medicinal plants in the traditional medical systems of many cultures. Many plants have been utilized without a clear understanding of their correct ingredients or activities as dietary adjuvants for a variety of disorders (Alqahtani *et al*., 2022). The increasing cost and side effects of synthetic hypoglycemic agents might be the reason for this approach. Even though a number of manufactured drugs have been developed for the therapy of type 2 diabetes, the standard for effective and safe treatment has not yet been established. Traditional plant remedies for diabetes have been suggested for investigation by the WHO because they are thought to be ideal candidates for oral medication, efficacious, non-toxic and have few or no adverse effects (Alam, 2021). Many plant species have been validated scientifically, demonstrating the effectiveness of botanicals in lowering blood sugar levels. As a result of publications on their possible efficacy in treating diabetes, it is believed that phytochemicals play a significant role in the treatment of the disease. However, further research is required to meet the need for naturally occurring medications and nutraceuticals.

Echinops ritro is a plant found mostly in Xinjiang, China, and is a species of the *Echinops* genus within the Compositae family. *Echinops grijsii* is replaced by it in traditional Uyghur medicine (Earles, 1973). Several bioactive substances found in the plant, including thiophenes, sesquiterpenes, alkaloids and flavonoids, have anti-fungal, anti-viral and anti-tumor properties, respectively (Zeng *et al*., 2011). There has been little study done recently on the entire plant, despite the fact that its root has been extensively researched (Li *et al*., 2019). The enzyme found in the small intestine that converts big carbohydrates into simple sugar is α-amylase. Blood glucose levels can be regulated by targeting this specific enzyme (Kaur *et al*., 2021). An essential computational technique in computer-aided drug design, especially for diabetes mellitus, is structure-based virtual screening (Chandershekar *et al*., 2020). Drug development is accelerated by the ability to identify potentially active molecules. Enzyme α-amylase is responsible for breaking down big carbs into smaller sugars; therefore, finding the right ligands for it is one way that molecular docking-based virtual screening helps manage diabetes mellitus (Tiwari *et al*., 2015).

MATERIALS AND METHODS

Protein retrieval and preparation (protein model preparation)

Target proteins α-amylase (PDB ID: 3BAJ) (Halim *et al*., 2024) were procured from the Protein Data Bank (PDB) database, accessible at (RCSB Protein Data Bank, 2026) and maintained by the Research Collaboratory for Structural Bioinformatics (RCSB) (Berman *et al*., 2000). The PDB ID was taken into consideration because of its superior structural quality as indicated by its percentile scores in global validation metrics, lower resolution (2.10 Å) and X-ray crystallographic structure. Schrodinger Maestro (version 12.5) was used to preprocess the protein structures (Rahman *et al*., 2022). The preprocessed proteins were then verified, optimized and energy-minimized in the OPLS3e force field utilizing the Schrodinger Maestro software (version 12.5) (Kumar *et al*., 2022).

Ligand extraction and preparation (library preparation)

An Overall 55 phytochemical bioactive substances, including rutin (Mc-55), Kaempferitrin (Mc-34), naringin (Mc-32) and Hyperoside (Mc-56), were chosen as ligands (Balabanova *et al*., 2023). These compounds were claimed to be derived from the plant *Bauhinia forficata*. The selected compounds were not experimentally extracted in this study. Instead, they were chosen based on literature reports of their occurrence in *Bauhinia forficata, Citrus spp.* and *Echinops ritro*. Drawings of the structure were made using SMILES from the PubChem database (PubChem, 2026). ChemDraw Professional 16.0 was used to draw the 2D structure. Chem-3D 16.0 was used to sketch the three-dimensional structures of these compounds. BIOVIA, or Discovery Studio Visualizer, was utilized to create the SDF file (Chakrabarti, 2023). The Schrodinger Maestro program (version 12.5), which uses OPLS3e as the default force field in LigPrep, was used to prepare the ligand structures.

Molecular docking

Schrodinger Maestro software (version 12.5) was used for molecular docking (Kalirajan *et al*., 2017) to investigate all possible orientations, conformations and binding affinities for the ligands with the α-amylase active site. The ligands were prepared in a suitable format for docking in Schrödinger Maestro (version 12.5) by converting them to SDF format using BIOVIA Discovery Studio Client 2021. The docking was performed using the previous protocol (Catania, 2023). The lead molecule was chosen based on the conformation that had the highest docking score (in kcal/mol). The top ten ligands were selected on the basis of scoring and then subjected to structural interaction fingerprinting (SIFt) analysis.

Structural interaction fingerprinting (SIFt) analysis

SIFt is a cutting-edge method for simulating and evaluating three-dimensional interactions between ligands and proteins. A binary digit interaction fingerprint is produced by the SIFt method, which translates the three-dimensional structural binding properties of a ligand-protein complex. Every fingerprint represents the "structural interaction pattern" of the complex, making it easier to arrange, examine and display large amounts of data inside ligand-

receptor complexes, which in turn makes database mining more effective (Mittal *et al*., 2021).

Pharmacokinetic parameters

Furthermore, the SwissADME (SwissADME, 2026) (Shakoor *et al*., 2024) tool was employed to forecast the pharmacokinetic characteristics (including absorption, distribution, metabolism, excretion, and toxicity - ADMET) of recently created compounds. This was done in order to assess the synthetic accessibility of the compounds. Toxicological analysis was conducted using two distinct servers, ProToxII (Shakoor *et al*., 2024) and StopTox (Borba *et al*., 2022). Drug target class and prediction of structurally related analogs (the prospective macromolecular targets of the best-selected candidates) were predicted using the Swiss Target Prediction service (Silva *et al*., 2021).

DFT studies (MESP/HOMO/LUMO analysis)

The conformational changes of four ligands (Mc -34, Mc -55, Mc -32, and Mc -56) of their co-crystallographic complexes with the 3BAJ structure were explored using the molecular electrostatic potential (MESP) approach using Gaussian, as per the previously reported protocol (Catania, 2023). Different electrostatic potential values were shown by these color differences at the molecule's surface. The areas (Fig. 1A) with a moderate reactivity range are colored in cyan, yellow and green intermediate tones.

RESULTS

Screening of phytochemicals via molecular docking

The results of this investigation showed that all 67 phytochemicals exhibited effective docking, with binding affinities ranging from -10.3 to -1.20 kcal/mol. Upon docking with α-amylase, the control Acarbose yielded a score of -13.3 kcal/mol (Table 1). Out of the phytochemicals tested, 59 (88%) had poor scores compared to the control Acarbose and only 8 (12%) were approved with a docking score better than - 9.5 kcal/mol, roughly. Among the recognized phytochemicals, Kaempferitrin (-10.3 kcal/mol) and rutin (-10.1 kcal/mol) had the highest binding affinity. The remaining eight recognized phytochemicals had binding affinities ranging from -9.6 to -9.1 kcal/mol. Yet, the 59 phytochemicals that were removed had binding affinities that ranged from -8.9 to -1.2 kcal/mol. Lupanine had the lowest binding affinity, measured -1.2 kcal/mol, as shown in table 1 and figs. 1B and 1C. Four final phytochemicals, such as Kaempferitrin (-10.3kcal/mol), rutin (- 10.1 kcal/mol), naringin (- 9.60 kcal/mol) and hyperoside (9.6kcal/mol), were processed through DFT and ADMET analysis based on high docking score.

Molecular docking analysis

A method for simulating interactions between tiny molecules and macromolecular targets is called "molecular docking." The (3BAJ) α-amylase is crucial for managing diabetes mellitus and blocking its function efficiently lowers blood glucose levels and wards off the disease. The preparation and validation of human pancreatic α-amylase (HPA) were done prior to molecular docking. With Discovery Studio Visualizer, the validity of the active site was verified. The catalytic region's identity as the ligand-binding region was confirmed by the presence of the TRP58, TRP59, TYR62, GLN63, ARG195, LYS200, GLU233, ILE235, GLU240, HIE299 and ASP300 residues in this region (Fig. 1A). Additionally, by re-docking the corresponding ligand, the target-an RMSD of less than 2 Å was verified (Fig. 1D). The RMSD computation and cognate ligand re-docking therefore corroborate the viability of the target protein for further analysis.

Significant findings were obtained from the analysis of molecular interactions between the target protein and the phyto ligands after visualization using BIOVIA Discovery Studio Visualizer. Every phytochemical exhibited both hydrophobic interactions and standard hydrogen bonding (Fig. 1A). Kaempferitrin exhibited interactions with the amino acid residues Trp-59, Tyr-62, His-101, Leu-162, Leu-165, Asp-197, Glu-233 and Asp-300 among the four top-scoring possibilities. Four conventional hydrogen bonds were established by this phytochemical with the residues Asp-300, Arg-195, Tyr-62 and Trp-59. In Van der Waals, only two residues Glu-233 and Leu-165-were linked to kaempferitrin. Rutin interacted with His-101, TyR-151, Asp-197, Leu-165, Lys-200, His-201, Glu-233, Glu-240 and Asp-300 in the second one. Amino acid residues Tyr-151, Glu-233, Lys-200, Asp-197 and Asp-300 formed typical hydrogen bonds. Pi-Alkyl interactions included two residues: His-101 and Leu-165.

Naringin, the third phytochemical, interacted with Trp-59, Tyr-62, Gln-63, Tyr-151, Leu-162, Asp-197, Arg-195, His-201, Glu-233 and Asp-300. Among these residues, seven established conventional hydrogen bonds: Tyr-62, Gln-63, Tyr-151, Arg-195, His-201, Glu-233 and Asp-300. Trp-59 is the lone residue that participates in the alkyl interaction. Hyperoside (D) is the fourth highest scoring ligand; it interacts with Pro-54, Trp-59, His-101, Leu-162, Thr-163, -Asp-197, Ala-198, Glu-233, Asp-300 and His-305. Three residue farm conventional hydrogen bonds with Hyperoside are found in Glu-233, Asp-300, Thr-163 and His-101, Ala-198 and Leu-162; these interactions reveal pi Alkyl interactions with Hyperoside. From the result, it can be seen that Kaempferitrin will be the best inhibitor for α-amylase because it makes three conventional hydrogen bonds with hotspot residue of active site of α-amylase as shown in fig. 1D. While Rutin makes a hydrogen bond with only two hotspot residues of the active site. Similarly, Nargrin and Hyperoside make hydrogen bonds with three and one hotspot residue of the protein pocket, respectively.

Structural interaction fingerprint (SIFt) analysis

This method was used to identify important residues that interact with ligands. All 54 ligands were docked with the active site of the α-amylase 3BAJ. The fingerprinting analysis shows that the residues ATRP-59, ATYR-62, ALEU-162, AARG-195, AASP-300 and AHES-305 were interacting with 82% of all ligand docked with α-amylase active site. This indicates that these residues are the hotspot residues of the binding cavity and can help to accommodate a potential inhibitor. Those phytochemicals which are showing more than 30% interaction with the hotspot residues will be good inhibitors. When 55 ligands were docked, they occupied the same binding cavity in protein as shown in fig. 1A. The quantification of contact, side chain, backbone, polar and hydrophobic interactions between the receptor (3BAJ) and the different ligands evaluated in this investigation is presented in fig. 2. The fig. 2 illustrate the interactions between residues A59-TRP, A62-TYR, A165-LEU, A197-ASH, A300-ASP and A305-HIE with the ligands. Based on the findings, it can be shown that A59-TRP, A62-TYR and 300-ASP were the most reactive residues with the compounds showing interaction through contact, side chain, hydrophobic interaction and backbone, as indicated by the bright orange hue. Residues A165-LEU and A197-ASH, shown in light green in Fig. 2, demonstrated contact, backbone, side-chain, polar and hydrophobic interactions. The residue A305-HIE is pale blue in color and exhibits contact, polar backbone, sidechain and hydrogen bond acceptor bond interactions with several ligands. According to the findings, the compounds Mc-34, Mc-55, Mc-32 and Mc-56 have the potential to be ligands with strong binding affinities, drug-like characteristics and a significant number of receptor contacts. As such, the current study has identified promising compounds with potential effectiveness in diabetes treatment. The ADMET investigations, which showed a notable degree of human absorption and a positive synthetic accessibility, corroborated this claim. The substances investigated in this work showed a remarkable capacity to interact with the residues of the 3BAJ active site, indicating a high binding affinity. Top binding ligands were selected, Mc-34, MC-55, Mc-32 and Mc-56, for further testing against the target protein 3BAJ. Protein-ligand interaction fingerprinting for ligands and hits extracted from the Schrödinger Suite 2020-2 library at residues linked to the interaction site within 4.0 Å. The contribution and absence of residues are denoted by the numbers 1 and 0, respectively. The hydrophobic, sidechain contact polar, backbone and H-bond acceptor qualities are used to color the residues. Residues with a 90% occupancy rate or above are deemed essential.

Drug likeness analysis

Analysis of drug likeness using ADME/T studies, various pharmacodynamic and pharmacokinetic features were assessed and all of the top candidates produced notable outcomes (Table 2). Of the four choices, Rutin has the largest molecular weight (610 g/mol). It was discovered that the intestinal absorption capacity of every phytochemical was reduced. No blood-brain barrier leakage was observed with any of the drugs. The four candidates were found to be soluble in water, indicating that the water solubility findings were good. Hyperoside had one infraction of the Lipinski and Ghose criteria, which were used to assess drug resemblance. The estimation was based on Lipinski's Rules of Five and the Ghose filter. Kaempferitrin, naringin and hyperoside demonstrated two violations each in Lipinski's Rules of Five, which was acceptable and they also followed the Ghose parameter with two violations. The bioavailability score of the top four ligands is all 0.17. The Pan-Assay Interference Compounds (PAINS) criteria disclosed one warning for rutin and hyperoside, zero alerts for kaempferitrin and nargrin and the same for Brank alerts. When taking into account the synthetic accessibility parameter, kaempferitrin performed better (6.48) than hproside (5.32), nargrin (6.16) and rutin (6.52). Two distinct servers were used to examine the toxicity parameters in order to ensure prediction reliability; both servers produced data that were consistent and adequate (Table 3). ProToxII server results with different parameters were notable. For every criterion and subcriterion on the ProToxII server, all four ligands showed an inactive state. With 100% accuracy, the toxicity class 5 of all four lead compounds was predicted to have an oral LD50 value of 5000 mg/kg. Rutin likewise had an inactive state for every parameter with the exception of one sub criterion, the immunotoxicity parameter of the Tox endpoints, which revealed a 50% likelihood of an active status. The four phytochemicals in the table were all determined to be safe and acceptable by the StopTox server after toxicity was assessed using five toxicity endpoints, including acute inhalation toxicity, acute oral toxicity, eye irritation and corrosion, skin sensitization and skin irritation and corrosion criteria were shown in table 4.

Frontier molecular orbital (FMOs)

The LUMO, HOMO and FMOs are the most significant orbitals in a molecule. These orbitals are crucial for understanding electron transport, chemical reactivity, stability and how a molecule interacts with other molecules. They are also relevant for optical, electric and quantum chemistry. Higher values of EHOMO indicate a stronger tendency of the molecule to give electrons. The HOMO energy defines a molecule's capacity to donate electrons. A molecule's capacity to receive electrons is determined by its electron-accepting potential (ELUMO); a lower ELUMO enhances the likelihood of an electron being accepted. Therefore, higher EHOMO and lower ELUMO values are what lead to a molecule's high reactivity and low stability. Table 5 shows the increasing order of the EHOMO values for the compounds under study: Naringin, rutin, hyperoside and kaempferitrin. Compared to other compounds, kaempferitrin (-0.327) has the greatest EHOMO value, indicating a greater propensity

to donate an electron to the target receptor. Table 5 also displays the computed ELUMO values. Compared to other compounds under study, Kaempferitrin has the lowest ELUMO value, showing its capacity to receive electrons. Moreover, as fig. 3A illustrates that both the EHOMO and ELUMO are completely dispersed throughout the molecular structure, indicating a substantial overlapping of HOMO-LUMO that would likely result in robust charge transfer behavior. When estimating a molecule's chemical reactivity, the band gap energy between the EHOMO and ELUMO is crucial. The stability and chemical reactivity of a molecule are reflected in its band gap energy levels. More stability, hardness and less reactivity are associated with greater band gap energies in molecules. Low stability and high reactivity are indicated by a reduction in the energy band gap. The energy band gap values are kaempferitrin <rutin <naringin <hyperoside, in that order. Kaempferitrin is more reactive at the target receptor than other compounds because it has the lowest band gap among the isolated molecules.

Molecular electrostatic potential (MESP)

Every ligand has a characteristic binding conformation that facilitates intermolecular interactions with its target protein, which are determined by the compound's stereo and electrical characteristics. Therefore, by identifying the molecular electronic characteristics responsible for a particular binding conformation of the ligand in a complex, it would assist in investigating the underlying molecular level factors accountable for their inhibitory efficacy. To better understand the impact of variations in the distribution of electrostatic potentials and the reactivity pattern on the binding affinity for α-amylase (3BAJ), MESPs were plotted on the highly active compounds Mc-34, Mc-55, Mc-32 and Mc-56 in this instance (Fig. 3B). Furthermore, Mulliken charge distributions of inhibitors with varying bioactivities against α-amylase (3BAJ) were computed at the B3LYP level to obtain a comprehensive understanding at the electronic level. The highly active molecule Mc-34 differs from Mc-55, Mc-32 and Mc-56 in terms of its electrical characteristics, as seen in table 5. Electronegative (red) and electropositive (blue) areas often appeared as regions that may either donate or accept electrons to the 3BAJ active site. Additionally, the docking data have indicated that the corresponding regions of Mc-34 may have a role in the significant interactions around the active site of 3BAJ with critical residues such as Trp-59, Tyr-62, His-101, Leu-162, Leu-165, Asp-197, Glu-233 and Asp-300. In addition, the MESP-identified electrical potential distribution is shown on Mc-34 (Fig. 3B). Comparably, the molecular electrostatic potential (MESP) of the other three top medications is determined using the same methodology and base sets, as shown in fig. 3B. The largest negative region in the MESP, colored red, represents the areas that electrophilic attacks prefer to target. Therefore, an attacking electrophile will be drawn to the negatively charged sites, whereas the blue areas will have the reverse effect. Given the sort of atoms and their electrical nature, it is evident that the medication affected the molecular size, shape and orientation of the negative, positive and neutral electrostatic potentials. The medication's binding affinity with the receptor at the active site may vary primarily due to differences in how the electrostatic potential is mapped around the drug. A map of the molecular electrostatic potential overlaid on a surface with a constant electron density displays the inhibitors of 3BAJ, Mc-34, Mc-55, Mc-32, and Mc-56, which are the active compounds (Fig. 3) The regions with green color show the potential midway between the two strongly electropositive and negative regions and have zero potential. Regions in dark blue represent the highly electropositive region, while regions in dark red indicate the very electronegative region.

DISCUSSION

The present study identified promising phytochemicals as potential inhibitors of human pancreatic α-amylase using a combined approach of molecular docking, SIFt, ADMET evaluation, FMO analysis and MESP mapping. Inhibiting α-amylase is an established strategy for controlling postprandial hyperglycemia in NIDDM and while synthetic agents like acarbose are effective, they often cause gastrointestinal side effects, prompting interest in plant-derived alternatives (Sales *et al*., 2012). Docking analysis revealed that most of the 67 tested phytochemicals had moderate to low affinities relative to acarbose; however, four compounds, Kaempferitrin, Rutin, Naringin and Hyperoside, stood out with docking scores better than -9.5 kcal/mol, Kaempferitrin being the most potent at -10.3 kcal/mol. Strong hydrogen bonding with key catalytic residues, particularly Trp-59, Tyr-62 and Asp-300, underpinned the higher affinity of Kaempferitrin, whereas Rutin interacted with slightly fewer hotspot residues. These findings align with earlier reports highlighting the significance of targeting conserved catalytic residues to achieve potent α-amylase inhibition (Martinez-Gonzalez *et al*., 2019).

SIFt analysis confirmed that residues such as Trp-59, Tyr-62, Leu-162, Arg-195 and Asp-300 were the most frequently contacted among high-affinity ligands, reflecting their role as structural hotspots in the active site. Kaempferitrin, Naringin and Rutin demonstrated high hotspot occupancy, consistent with the idea that efficient inhibitors combine strong binding energies with diverse non-covalent interactions to ensure stability within the binding pocket (Rasouli *et al*., 2017). ADMET profiling showed all four top candidates had favorable toxicity profiles, falling under Class 5 oral toxicity, with no blood-brain barrier penetration beneficial for avoiding central side effects. However, their low intestinal absorption, likely due to high polarity and glycosylation, may necessitate formulation strategies to improve bioavailability (Hu *et al*., 2025).

Table 1: Ligand library of natural products with docking score.

Source of inhibitor	Inhibitor	Binding affinities (kcal/mol)
Bauhinia forficate	Kaempferitrin	-10.3
Echinops ritro L	Rutin	-10.1
Citrus spp.	Naringin	-9.7
Echinops ritro L	Hyperoside	-9.6
Anemarrhena asphodeloides	Mangiferin	-9.5
Echinops ritro L	Isorhamnetin-3-O-Rutinoside	-9.5
Ficus bengalensis	Leucodelphinidin	-9.5
Echinops ritro L	Isoquercitrin	-9.1
Lupinus prunophilus	Lupanine	-1.20
Standard	Acarbose	-13.3
Bauhinia forficate	Kaempferitrin	-10.3

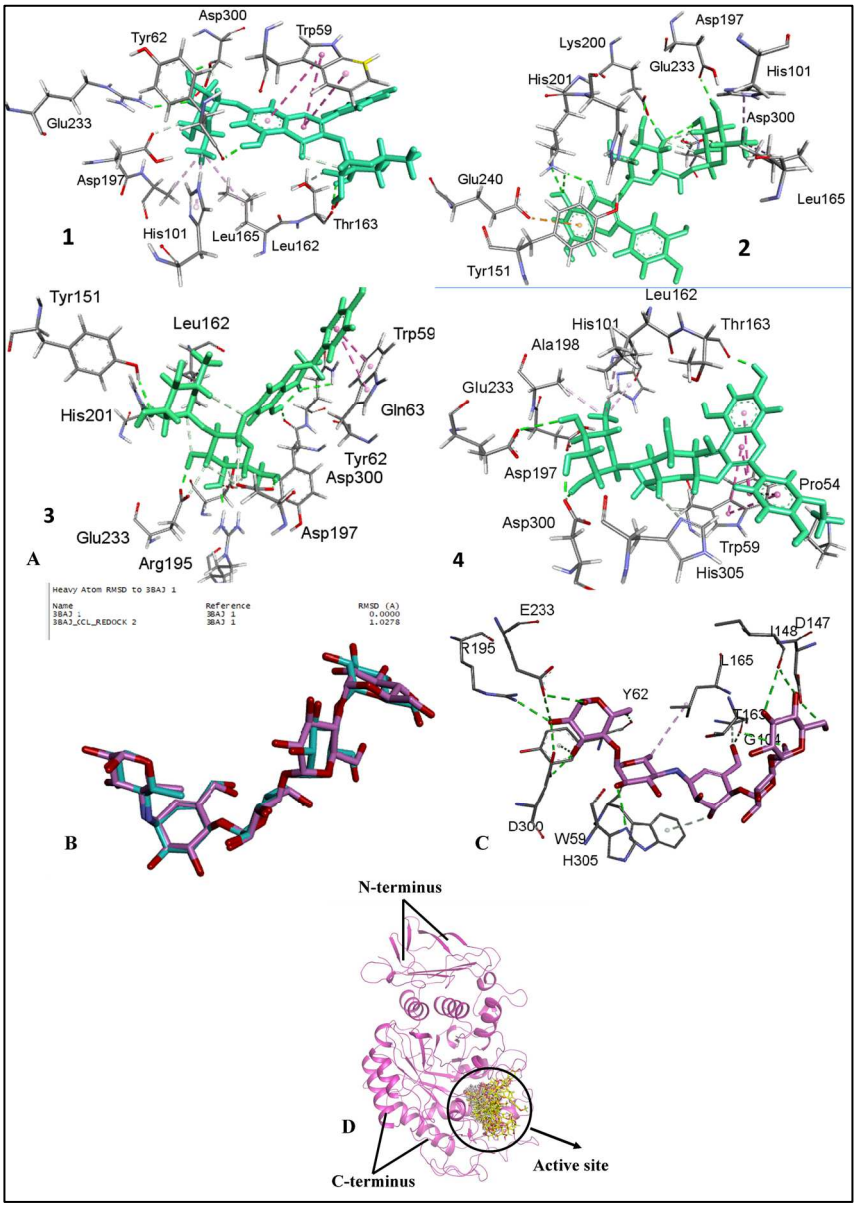

Fig. 1: (A) The interaction of top four ligands with pocket of (3BAJ) (1) Kaempferitrin, (2) Rutin and (3) Nargrin; (4) Hyperoside; (B) Three-dimensional (3D) image of the control ligand (CCL) with redock ligand; (C) α-amylase pocket (3BAJ); (D) The image of the docked ligands with protein (3BAJ) pocket.

Table 2: Evaluation of drug candidacy of Kaempferitrin, Rutin, Naringin and Hyperoside via ADME analysis.

Parameters		Kaempferitrin	Rutin	Naringin	Hyperoside
Physicochemical properties	MW	578	610	580	464
	Heavy atom	41	43	41	33
	Aromatic heavy atom	16	16	12	16
	fraction csp3	0.44	0.44	0.52	0.29
	rotatable bonds	5	6	6	4
	H-bond acceptor	14	16	14	12
	H-bond DONOR	14	10	8	8
	MR	137.93	141	134.9	110
	TSPA	228	269	225	210
Lipophilicity	iLOGP	2.44	0.46	1.96	1.45
	XLOGP3	-0.09	-0.33	-0.44	0.36
	WLOGP	-0.72	-1.69	-1.49	-0.54
	MLOGP	-2.69	-3.89	-2.77	-2.59
	Silicon-IT Log P	-1.04	-2.11	-1.64	-0.59
	Consensus log P	-0.42	-1.51	-0.87	-0.38
Water solubility	ESOL Log S	-3.33	-3.3	-2.89	-3.04
	Ali Log S	-4.27	-4.87	-3.82	-4.35
	SilicoS-IT Log SW	-1.46	-0.29	-0.49	-1.51
	Log Kp (em/s)	-9.89	-10.26	-10.15	-8.88
Drug likeness	Lipinski violation	2	2	2	1
	Ghose violation	2	2	2	1
	Veber violation	1	1	1	1
	Egan violation	1	1	1	1
	Muegge violation	3	4	3	3
	Bioavailability score	0.17	0.17	0.17	0.17
Medicinal chemistry	Pain alert	0	1	0	1
	Brank alert	0	1	0	1
	Lead-likeness violation	1	1	0	0
	Synthetic accessibility	6.48	6.52	6.16	5.32
	LIGANDS	Mc-34	Mc-55	Mc-32	Mc-56

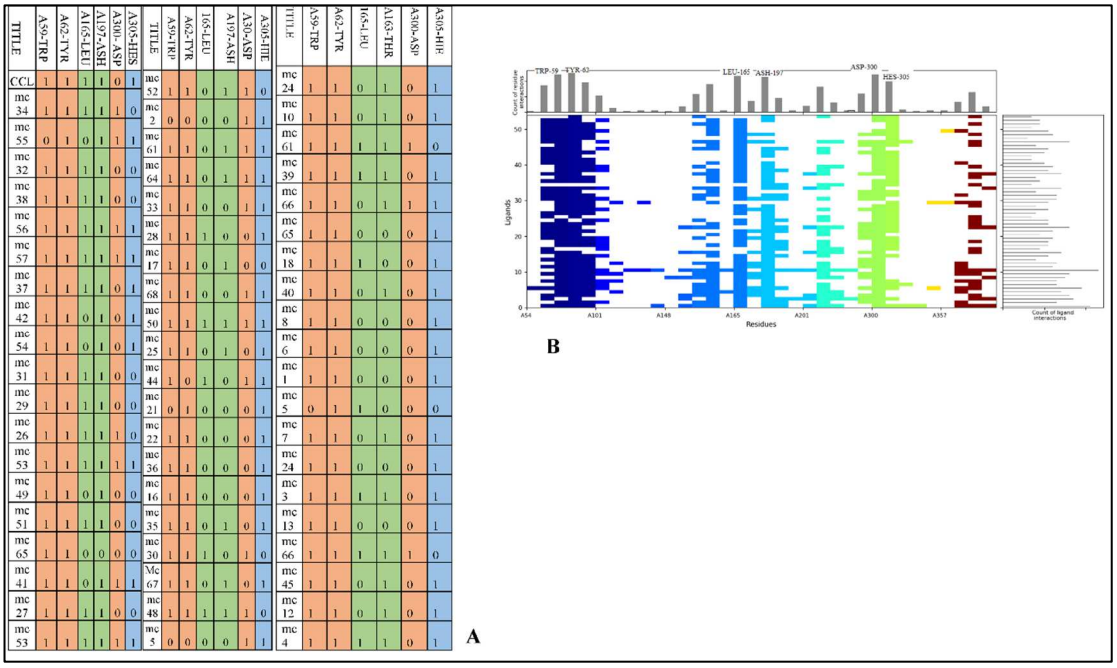

Fig. 2: (A) Structural interaction fingerprinting (SIFt) analysis; (B) Protein-ligand interaction fingerprints.

Table 3: Toxicity analysis for Kaempferitrin, Rutin, Naringin and Hyperoside.

Classification	Target	Mc-34		MC-55		Mc-32		Mc-56	
		Pre	Pro	Pre	Pro	Pre	Pro	Pre	Pro
Organ toxicity	Hepatotoxicity	I	0.73	A	0.69	I	0.81	I	0.82
Toxicity endpoint	Carcinogenicity	I	0.53	I	0.62	I	0.90	I	0.85
	Immunotoxicity	A	0.94	A	0.96	A	0.99	A	0.66
	Mutagenicity	I	0.68	I	0.97	I	0.73	I	0.76
	Cytotoxicity	I	0.92	I	0.93	I	0.66	I	0.69
Tox21-Nuclear receptor signaling pathways	AhR	A	0.55	I	0.97	I	0.88	I	0.92
	AR	I	0.98	I	0.99	I	0.96	I	0.90
	AR-LBD	I	0.93	I	0.96	I	0.99	I	0.98
	Aromatase	I	0.94	A	1	I	1	I	1
	ER	I	0.71	NC	NC	I	0.94	I	0.91
	ER-LBD	I	0.82	A	1	I	0.99	I	0.99
	PPAR-GAMMA	I	0.93	I	0.99	I	0.99	I	0.99
Tox21-Stress response pathways	HSE	I	0.90	I	0.88	I	0.99	I	0.98
	HSE	I	0.90	I	0.88	I	0.99	I	0.98
	MMP	I	0.53	I	0.70	I	0.99	I	0.98
	p53	I	0.81	I	0.96	I	0.75	A	0.50
	ATAD5	I	0.72	I	0.99	I	0.99	I	1

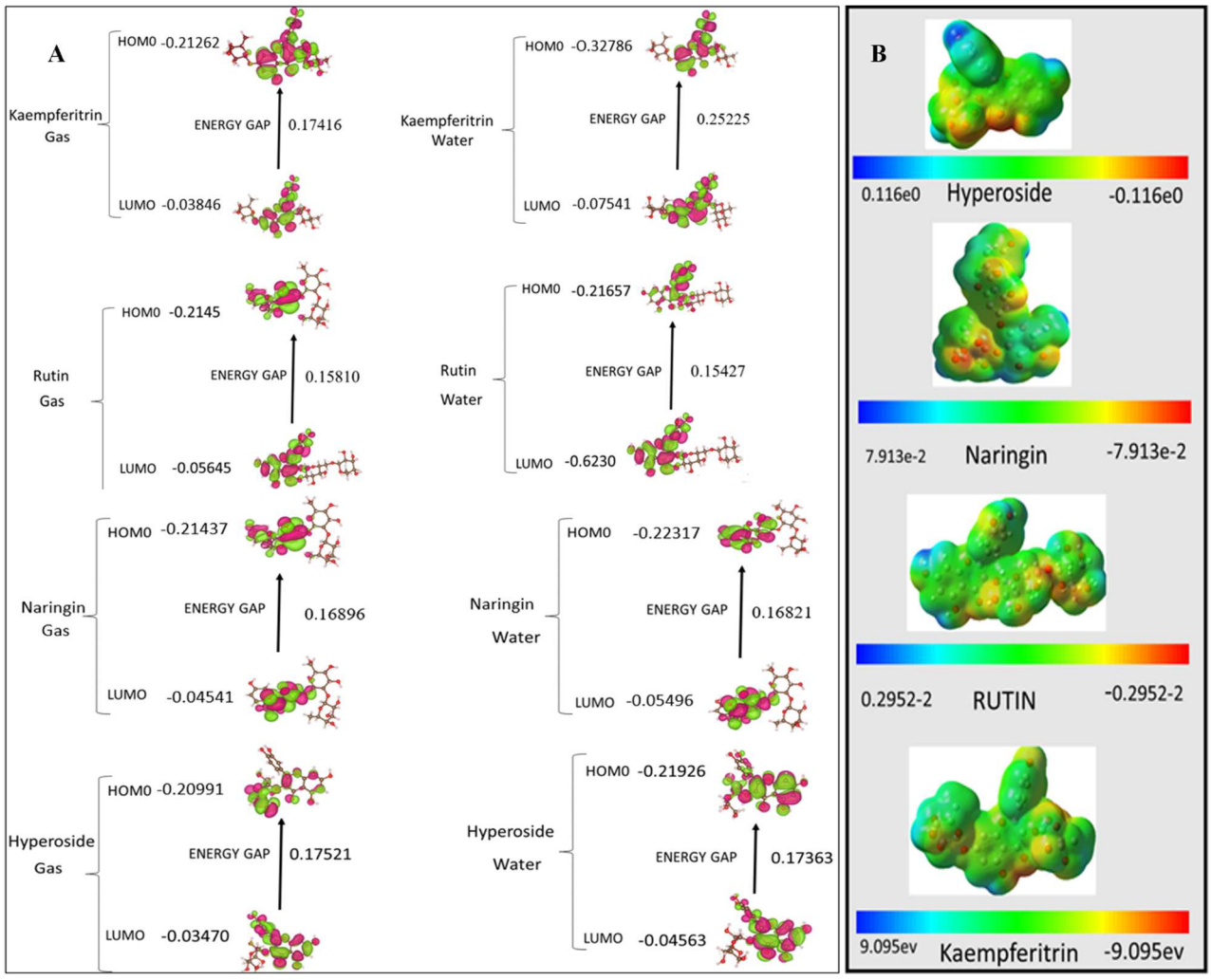

Fig. 3: (A) The Homo and Lumo of top 4 scoring ligands; (B) MESP surface of the top 4 phytochemicals.

Table 4: Stop tox values of top 4 scoring ligands.

Ligands	Acute inhalation toxicity	Acute oral toxicity	Acute dermal toxicity	Eye irritation and toxicity	Skin sensitization	Skin irritation and corrosion
Mc-34-T1	Non-toxic	Non toxic	Non toxic	Non toxic	Non-sensitizer	Negative
Mc-55-T2	Non-toxic	Non toxic	Non toxic	Non toxic	Non-sensitizer	Negative
Mc-32-T3	Non-toxic	Non toxic	Non toxic	Non toxic	Non-sensitizer	Negative
Mc-56-T4	Non-toxic	Non toxic	Non toxic	Non toxic	Non-sensitizer	Negative

Table 5: HOMO (eV), LUMO (eV), dipole moment (Debye), energy gap ΔE (eV), ionization potential IP (eV), electron affinity EA (eV), electronegativity χ (eV), chemical potential μ (eV), global hardness η (eV), and global softness S (eV-[1]) of the top four ligands in gas and aqueous phases.

Ligand	Phase	HOMO	LUMO	Dipole Moment	ΔE	IP	EA	χ	μ	η	S	ΔE
Mc-34-T1	Gas	-0.21262	-0.03846	4.2622	0.17416	0.21262	0.03846	0.12554	-0.12554	0.08708	11.48	0.0905
Mc-34-T1	Water	-0.32766	-0.0754	6.3075	0.25225	0.32766	0.07541	0.20154	-0.20154	0.12612	7.93	0.16104
Mc-55-T2	Gas	-0.21455	-0.0564	6.5645	0.15810	0.21455	0.05645	0.13550	-0.13550	0.07905	12.65	0.1162
Mc-55-T2	Water	-0.21657	-0.06230	8.4274	0.15427	0.21657	0.06230	0.13944	-0.13944	0.07714	12.96	0.1261
Mc-32-T3	Gas	-0.21437	-0.04541	2.2229	0.16896	0.21437	0.04541	0.12989	-0.12989	0.08448	11.84	0.0998
Mc-32-T3	Water	-0.22317	-0.05496	2.7515	0.16821	0.22317	0.05496	0.13907	-0.13907	0.08411	11.89	0.1149
Mc-56-T4	Gas	-0.20991	-0.03470	7.4769	0.17521	0.20991	0.03470	0.12231	-0.12231	0.08760	11.41	0.0870
Mc-56-T4	Water	-0.21926	-0.04563	9.7539	0.17363	0.21926	0.04563	0.13245	-0.13245	0.08682	11.52	0.17363

(ΔE); Energy gap, IP; Ionization potenetial, EA; Electron Affinity, χ; Electronegativity, μ; Electrochemical Potential, η; Hardness, S; Softness, (ΔE); Electrophilicity

Electronic property analysis using FMOs provided further mechanistic insight. Kaempferitrin's high EHOMO and low ELUMO values suggested a strong capacity for both electron donation and acceptance, potentially facilitating charge transfer with active site residues. Its low HOMO-LUMO gap indicated higher reactivity, consistent with adaptable binding in dynamic protein environments. This relationship between quantum descriptors and biological activity has been observed in prior flavonoid-enzyme studies. MESP mapping revealed complementary electrostatic patterns between potent ligands and the α-amylase active site. Electronegative regions on Kaempferitrin and Rutin aligned with positively charged residues, while electropositive areas matched negatively charged catalytic residues such as Asp-197 and Glu-233. Such electrostatic complementarity is a known determinant of stable enzyme-inhibitor complexes (Kumar *et al*., 2011).

Overall, Kaempferitrin and Rutin emerge as strong candidates for further *in-vitro* and *in-vivo* evaluation. The multi-parameter computational evidence spanning binding affinity, hotspot interactions, pharmacokinetics and electronic complementarity support their potential as natural alternatives to synthetic α-amylase inhibitors. Further work should focus on kinetic assays, crystallographic confirmation and delivery optimization to address absorption limitations, thereby advancing these compounds toward application in glycemic control.

CONCLUSION

The current study highlights the potential of Kaempferitrin as an exceptionally powerful natural suppressor of NIDDM through its α-amylase inhibitory abilities. Among the compounds screened, kaempferitrin displayed the best binding affinity (-10.3 kcal/mol) towards α-amylase and showed especially strong interactions with the active site residues of the enzyme. This interaction with key hotspot residues was also supported by SIFt analysis. The best four compounds, Kaempferitrin, Rutin, Naringin and Hyperoside, had good drug-likeness, good ADME profile, and low toxicity risk. DFT and Mulliken charge analyses supported their chemical stability and reactivity, with kaempferitrin standing out due to its strong electron-donating and accepting properties, as well as the lowest energy gap, indicating higher reactivity at the target site. These findings collectively show that kaempferitrin combined with Rutin, naringin and hyperoside offer potential leads in developing plant-based antidiabetic drugs. However, experimental validations are essential to verify the computational insights.

Acknowledgements

The authors are grateful to the Institute of Pharmaceutical Sciences (IPS), University of Veterinary and Animal Sciences (UVAS), Lahore, Pakistan, for providing computational facilities and academic support for this study.

Authors' contributions

Mujahid Jalal and Muhammad Hasnat: Contributed to conceptualization, molecular docking analysis and data interpretation; Ayisha Khalid and Talha Ali Chohan: Contributed to methodology development and computational analysis; Ashfaq Ahmad and Ayesha Riaz: Assisted in data analysis and manuscript drafting; Sobia Alyas and Muhammad Shoaib Ali Gill: Participated in data validation and literature review; Umair Khurshid and Anjum Khursheed: Contributed to pharmacokinetic and toxicity analysis; Tahir Ali Chohan: Assisted in visualization and figure preparation; Sirajudheen Anwar and Hammad Saleem: Supervised the study, contributed to study design, interpretation of results and final manuscript revision. All authors read and approved the final manuscript.

Funding
There was no funding.

Data availability statement
The datasets generated and analyzed during the current study are included within the manuscript. Additional data related to the computational analyses are available from the corresponding author upon reasonable request.

Ethical approval
This study was conducted entirely using computational and *in-silico* methods and did not involve human participants, animal experiments or clinical samples. Therefore, ethical approval was not required.

Conflict of interest
The authors declare no conflicts of interest.

REFERENCES

Alam MM (2021). Prevalence of type 2 diabetes mellitus complications in human. Doctoral dissertation, *Chattogram Veterinary & Animal Sciences University*.

Alqahtani AS, Ullah R and Shahat AA (2022). Bioactive constituents and toxicological evaluation of selected antidiabetic medicinal plants of Saudi Arabia. *Evid. Based Complement. Alternat. Med.,* **2022**(1): 7123521.

Balabanova V, Zheleva-Dimitrova D, Voynikov Y, Zengin G, Joubert O and Gevrenova R (2023). New insight into enzyme inhibitory and anti-proliferative activity of Echinops ritro L.(Asteraceae). *Proc. Bulg. Acad. Sci.,* **76**(12): 1893-1902.

Berman HM, Westbrook J, Feng Z, Gilliland G, Bhat TN, Weissig H, Shindyalov IN and Bourne PE (2000). The protein data bank. *Nucleic. Acids Res.,* **28**: 235-242.

Borba JV, Alves VM, Braga RC, Korn DR, Overdahl K, Silva AC, Hall SU, Overdahl E, Kleinstreuer N and Strickland J (2022). STopTox: An *in-silico* alternative to animal testing for acute systemic and topical toxicity. *Environ. Health Perspect.,* **130**(2): 027012.

Catania KM (2023). Design, identification and validation of calcium adenosine triphosphatase isoform 2a (SERCA2a) receptor modulators: A novel drug target for the treatment of heart failure. Master's thesis, University of Malta.

Chakrabarti M (2023). Revolutionizing antimicrobial drug discovery: Computational design and admet studies of emerging potent anti-microbial agents. *Int. J. Pharm. Pharm. Sci.*, **15**(8): 28-35.

Chandershekar A, Bhaskar A, Mekkanti MR and Rinku M (2020). A Review on computer aided drug design (Caad) and it's implications in drug discovery and development process. *Int. J. Health Care Biol. Sci.*, **1**(1): 27-33.

Classification and Diabetes DO (2020). Standards of medical care in diabetes-2020. *Diabetes Care,* **43**: S14-S31.

Earles M (1973). Chinese Pharmacopoeia. pp. 99–100.

Halim SA, Lodhi HW, Waqas M, Khalid A, Abdalla AN, Khan A and Al-Harrasi A (2024). Targeting α-Amylase enzyme through multi-fold structure-based virtual screening and molecular dynamic simulation. *J. Biomol. Struct. Dyn.,* **42**: 5617-5630.

Hu L, Luo Y, Yang J and Cheng C (2025). Botanical flavonoids: Efficacy, absorption, metabolism and advanced pharmaceutical technology for improving bioavailability. *Molecules,* **30**: 1184.

Kalirajan R, Sankar S, Jubie S and Gowramma B (2017). Molecular docking studies and *in-silico* ADMET screening of some novel oxazine substituted 9-anilinoacridines as topoisomerase II inhibitors. *Indian J. Pharm. Educ. Res.*, **51**: 110-115.

Kaur N, Kumar V, Nayak SK, Wadhwa P, Kaur P and Sahu SK (2021). Alpha-amylase as molecular target for treatment of diabetes mellitus: A comprehensive review. *Chem. Biol. Drug Des.,* **98**: 539-560.

Kumar M, Roy A, Rawat RS, Alok A, Tetala KK, Biswas NR, Kaur P and Kumar S (2022). Identification and structural studies of natural inhibitors against SARS-CoV-2 viral RNA methyltransferase (NSP16). *J. Biomol. Struct. Dyn.,* **40**: 13965-13975.

Kumar R, Saha P, Kumar Y, Sahana S, Dubey A, Prakash OJWJO (2020). A review on diabetes mellitus: Type 1 & Type 2. *World J. Pharm. Sci.*, **9**: 838-850.

Kumar S, Narwal S, Kumar V and Prakash O (2011). α-glucosidase inhibitors from plants: A natural approach to treat diabetes. *Pharmacogn. Rev.*, **5**: 19.

Li LB, Xiao GD, Xiang W, Yang X, Cao KX and Huang RS (2019). Novel substituted thiophenes and sulf-polyacetylene ester from echinops ritro L. *Molecules,* **24**: 805.

Martinez-Gonzalez AI, Diaz-Sanchez A, De La Rosa L, Bustos-Jaimes I and Alvarez-Parrilla E (2019). Inhibition of α-amylase by flavonoids: Structure activity relationship (SAR). *Spectrochim. Acta A Mol. Biomol. Spectrosc.*, **206**: 437-447.

Mehrpour O, Saeedi F, Hoyte C, Hadianfar A, Nakhaee S and Brent J (2022). Distinguishing characteristics of exposure to biguanide and sulfonylurea anti-diabetic medications in the United States. *Am. J. Emerg. Med.*, **56**: 171-177.

Mittal L, Kumari A, Srivastava M, Singh M and Asthana S (2021). Identification of potential molecules against COVID-19 main protease through structure-guided virtual screening approach. *J. Biomol. Struct. Dyn.,* **39**: 3662-3680.

PubChem (2026). PubChem database. Available at: https://pubchem.ncbi.nlm.nih.gov/ (Accessed 13 March 2025).

Rahman MH, Biswas P, Dey D, Hannan MA, Sahabuddin M, Araf Y, Kwon Y, Emran TB, Ali MS and Uddin MJ (2022). An *in-silico* identification of potential flavonoids against kidney fibrosis targeting TGFβR-1. *Life,* **12**: 1764.

Rasouli H, Hosseini-Ghazvini SMB, Adibi H and Khodarahmi R (2017). Differential α-Amylase/α-glucosidase inhibitory activities of plant-derived phenolic compounds: A virtual screening perspective for the treatment of obesity and diabetes. *Food Funct.*, **8**: 1942-1954.

RCSB Protein Data Bank (2026). RCSB PDB. Available at: https://www.rcsb.org/ (Accessed 15 April 2025).

Sales PM, Souza PM, Simeoni LA, Magalhaes PO and Silveira D (2012). α-amylase inhibitors: a review of raw material and isolated compounds from plant source. *J. Pharm. Pharm. Sci.*, **15**: 141-183.

Shakoor B, Yaqoob N, Shafiq N, Bin Jardan YA, Nafidi HA and Bourhia M (2024). *In-silico* ADME/Tox profiling of mushroom secondary metabolites. *Chemistry*, **9**: e202304312.

Silva GM, Borges RS, Santos KL, Federico LB, Francischini IA, Gomes SQ, Barcelos MP, Silva RC, Santos CB and Silva CH (2021). Revisiting the proposition of binding pockets and bioactive poses for GSK-3β allosteric modulators addressed to neurodegenerative diseases. *Int. J. Mol. Sci.*, **22**: 8252.

SwissADME (2026). SwissADME. Available at: http://www.swissadme.ch (Accessed 10 April 2025).

Tiwari S, Srivastava R, Singh C, Shukla K, Singh R, Singh P, Singh R, Singh N and Sharma R (2015). Amylases: An overview with special reference to alpha amylase. *J. Global Biosci.*, **4**: 1886-1901.

Tomic D, Shaw JE and Magliano DJ (2022). The burden and risks of emerging complications of diabetes mellitus. *Nat. Rev. Endocrinol.*, **18**: 525-539.

Wang H, Li N, Chivese T, Werfalli M, Sun H, Yuen L, Hoegfeldt CA, Powe CE, Immanuel J and Karuranga S (2022). IDF diabetes atlas: Estimation of global and regional gestational diabetes mellitus prevalence for 2021 by international association of diabetes in pregnancy study group's criteria. *Diabetes Res. Clin. Pract.,* **183**: 109050.

Zeng X, Qiu Q, Jiang C, Jing Y, Qiu G and He X (2011). Antioxidant flavanes from *Livistona chinensis*. *Fitoterapia,* **82**(4): 609-614.